

Reflection symmetry instability at high spins in $^{162,164}\text{Yb}$

R. G. Nazmitdinov,^{1,2} J. Kvasil,³ and A. Tsvetkov³

¹*Departament de Física, Universitat de les Illes Balears, E-07122 Palma de Mallorca, Spain*

²*Bogoliubov Laboratory of Theoretical Physics, Joint Institute for Nuclear Research, 141980 Dubna, Russia*

³*Institute of Particle and Nuclear Physics, Charles University,*

V.Holešovičkách 2, CZ-18000 Praha 8, Czech Republic

(Dated: February 6, 2020)

A shape evolution of $^{162,164}\text{Yb}$ in yrast states is traced using the self-consistent Skyrme Hartree-Fock calculations. We found that nonaxial octupole deformations (in particular, Y_{31} term) become favorable at $\hbar\Omega > 0.4\text{MeV}$ in ^{162}Yb , while in ^{164}Yb a nonaxial quadrupole shape is dominant at fast rotation. The cranked Nilsson model and random phase approximation are used to understand the dynamics of octupole correlations in both nuclei. We demonstrate that the disappearance of one of the octupole vibrational modes in the rotating frame gives rise to the nonaxial octupole deformations in ^{162}Yb , while the octupole modes are nonzero in ^{164}Yb .

PACS numbers: 21.10.Re, 21.60.Jz, 27.70.+q

Shell structure plays a prominent role in the formation of ground and excited nuclear states. It is crucially important at fast rotation, when nuclear stability against fission is determined by a delicate balance of different constituents of a nuclear potential. In a geometrical approach [1], where the concept of shape deformation is one of the basic cornerstones, effects produced by quadrupole degrees of freedom are well understood for various effective potentials. Whether octupole degrees of freedom are of any importance and how they are manifested, – these questions stimulate a noticeable fraction of experimental efforts in high spin physics [2].

Numerous calculations exploiting the intrinsic reflection symmetry breaking of a nuclear mean field predict the existence of stable axial octupole deformation in the ground state for Ra-Th ($Z \sim 88$, $N \sim 134$) and Ba-Sm ($Z \sim 58$, $N \sim 88$) nuclei, where strong octupole instability is due to the coupling of $j_{15/2} - g_{9/2}$, $i_{13/2} - f_{7/2}$, $h_{11/2} - d_{5/2}$ orbitals [3]. The potential energy surface produced by different calculations is, however, quite shallow. Experimental nuclear spectra also show a pronounced parity splitting at low angular momenta. Rather dynamical octupole effects (vibrations) are dominant over static effects (octupole deformations) at low spins. The increase of the angular momentum decreases pairing correlations which reduce the octupole interaction, since they couple the orbitals with the same parity. With rotation, the density of different parity states is enhancing markedly near the Fermi level. Indeed, one observes a smooth decrease of the parity splitting with the increase of the rotational frequency fairly in a few nuclei. These features are nicely reproduced within the cranking+Hartree-Fock-Bogoliubov (HFB) approach with Gogny forces in Ba-Sm region [4]. Similar calculations with Skyrme [5] and Gogny [6] forces predict a nonaxial Y_{31} octupole deformation in light nuclei at high spins. The results based on the Skyrme interaction demonstrate the importance of a nonaxial Y_{32} octupole deformation in actinide nuclei at fast rotation [7]. Notice that rotation induces the contribution of nonaxial quadrupole and octupole components

of effective nuclear potentials.

A wealth of experimental information accumulated in the past few years on high spin states in the transitional nuclei $Z \sim 70$, $N \sim 90$ prompted us to investigate the question to what extent dynamical octupole effects observed at low spins in this mass region might develop static octupole deformations at sufficiently high angular momenta. This is a main subject of this Letter.

To analyse the rotational evolution of equilibrium deformations we have employed the HFODD code [8]. In the present calculations the pairing correlations are neglected, since they are not expected to play an important role at large rotational frequencies. Our HF calculations based on the cranked Skyrme SKP interaction (see details in Ref.7) demonstrate that a spontaneous symmetry breaking phenomenon occurs in ^{162}Yb at large rotational frequencies (see Fig.1). The mean field solution with a

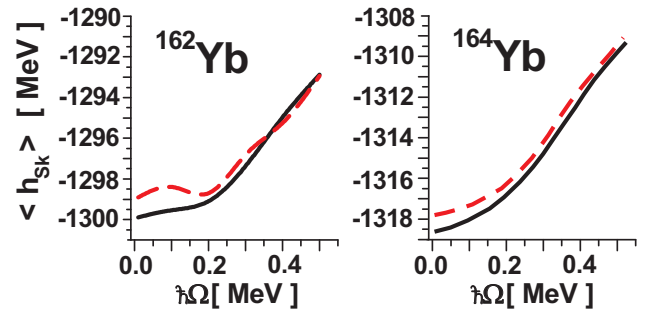


FIG. 1: (Color online) The rotational evolution of the SkP Skyrme mean field energy: pure nonaxial quadrupole (solid line) and nonaxial quadrupole+octupole (dashed line) solutions.

broken reflection symmetry (with nonzero $\langle Q_{30} \rangle$, $\langle Q_{31} \rangle$ momenta and a small admixture of $\langle Q_{32} \rangle$ one, see Fig.2) becomes favorable at $\hbar\Omega > 0.4\text{MeV}$, in contrast to the solution with a reflection symmetry. In ^{164}Yb both the minimal solutions are very close to each other, while the pure quadrupole one determines properties of yrast states

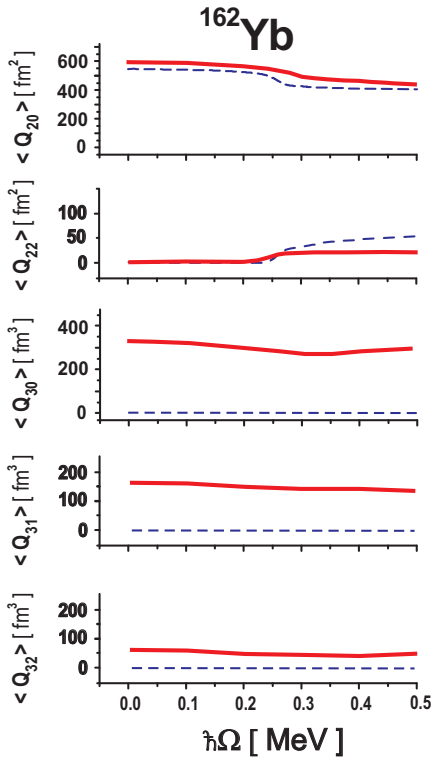


FIG. 2: (Color online) The rotational behaviour of quadrupole ($\langle Q_{2m} \rangle$) and octupole ($\langle Q_{3m} \rangle$) momenta for a broken (solid line) and an unbroken (dashed line) reflection symmetry SkP Skyrme mean field solutions for ^{162}Yb .

at fast rotation. Hereafter, $\langle \dots \rangle$ means the averaging over the mean field vacuum (yrast) state at a given rotational frequency Ω . We obtain a similar pattern with the SKIII parametrisation, which conforms our main finding, however, with slightly higher values of the energy minima. At slow rotation $\hbar\Omega \leq 0.3\text{MeV}$ (when pairing is important) the results should be taken cautiously, while the calculations provide a most credible tendency at $\hbar\Omega > 0.3\text{MeV}$.

A transparent physical idea that an instability of a nuclear potential with respect to a given deformation implies a softening of the corresponding vibrational mode [1] enables us to shed light on the mean field results. The cranked shell model that incorporates a random phase approximation (RPA) represents a powerful tool to illuminate dynamics of various correlations, evolving from shape fluctuations (vibrations) to a nuclear shape instability. We use a CRPA approach [9] that consists in a self-consistent solution of the cranked Nilsson potential for the yrast line and analysis of the low-lying excitations near the yrast line in the RPA. Our consideration is based on the Hamiltonian

$$\hat{H}_\Omega = \hat{H}_0 - \sum_\tau \lambda_\tau \hat{N}_\tau + V - \Omega \hat{J}_x. \quad (1)$$

The term $\hat{H}_0 = \hat{H}_N + \hat{H}_{\text{add}}$ contains the Nilsson Hamiltonian \hat{H}_N with quadrupole deformations and the additional term that restores the local Galilean invariance

of the Nilsson potential, broken in the rotating frame. To describe different parity states, the interaction V includes separable monopole pairing, monopole-monopole, quadrupole-quadrupole and spin-spin terms for the positive parity ($\pi = +$) and dipole-dipole, octupole-octupole terms for the negative parity ($\pi = -$). The chemical potentials λ_τ ($\tau = n$ or p) are determined so as to give correct average particle numbers $\langle \hat{N}_\tau \rangle$. All multipole and spin-multipole operators have a good isospin T and signature $r = \pm 1$ (see the properties of the matrix elements in Ref.10). They are expressed in terms of doubly stretched coordinates $\tilde{x}_i = (\omega_i/\omega_0) x_i$, which ensure the self-consistent conditions at the equilibrium deformation. All the details of this approach are thoroughly discussed in Ref.9. Although the CRPA approach is based on the Nilsson potential, it contains static and dynamic effects induced by rotation and serves a useful purpose of independent view of the Skyrme results.

The mode associated with the rotation about the x -axis determines the Thouless-Valatin moment of inertia \mathcal{J}_{TV}

$$[\hat{H}_\Omega(\pi_{r=\pm}), i\hat{\Phi}] = \frac{\hat{J}_x}{\mathcal{J}_{TV}}, \quad [\hat{\Phi}, \hat{J}_x] = i. \quad (2)$$

Here, $\hat{H}_\Omega(\pi_{r=\pm})$ is the positive signature term of the full Hamiltonian; an angle operator $\hat{\Phi}$ is the canonical partner of the angular momentum operator \hat{J}_x . The solution of these equations leads to the definition $\mathcal{J}_{TV} = \det A / \det B$ where the matrix $A(B)$ has a dimension $n = 10(11)$ due to a coupling of different operators involved in $\hat{H}_\Omega(\pi_{r=\pm})$ [9]. We recall that a comparison of the dynamical moment of inertia $\mathcal{J}^{(2)} = -d^2E/d\Omega^2$ ($E = \langle \hat{H}_\Omega \rangle$) with the Thouless-Valatin \mathcal{J}_{TV} moment of inertia calculated in the RPA provides a faithful test of the self-consistency of a cranking microscopic theory. The equivalence between these momenta of inertia certainly holds, if one found a self-consistent mean field minimum and spurious solutions are separated from the physical ones (see exact results for a solvable model in Ref.11). The use of the phenomenological rotational dependence of the gap parameter near the backbending region (see Ref.9), the ls and l^2 terms of the Nilsson potential affect this equivalence. However the result achieved in our calculations yields a reasonable self-consistency (see Fig.3). We obtain a good agreement between our results and experimental kinematic $\mathfrak{S}_{exp,\nu}^{(1)}(\Omega(I)) = \hbar^2 2I / (E_\nu(I+1) - E_\nu(I-1))$ and the dynamic $\mathfrak{S}_{exp,\nu}^{(2)} = \hbar dI/d\Omega = 2\hbar / (\Omega_\nu(I+1) - \Omega_\nu(I-1))$ momenta of inertia for the yrast states. Here, $E_\nu(I)$ is an experimental energy for the rotational band ν ($\nu = \text{yrast}, \beta, \gamma, \dots$) [12]. The drastic change of the kinematic momenta of inertia starts slightly earlier and ends slightly later than in experiments. It is known that in the backbending region the cranking approach is less reliable [13]. Nevertheless, one observes a similar rotational dependence of the magnitude of the calculated and experimental kinematic momenta of inertia till $\sim 0.6\text{MeV}$

in ^{164}Yb , while a good agreement holds till $\sim 0.45\text{MeV}$ in ^{162}Yb (see below). The results for the dynamic momenta of inertia reproduce with a reasonable accuracy the fluctuations in the backbending region, in spite of the approximations made in our approach. The consis-

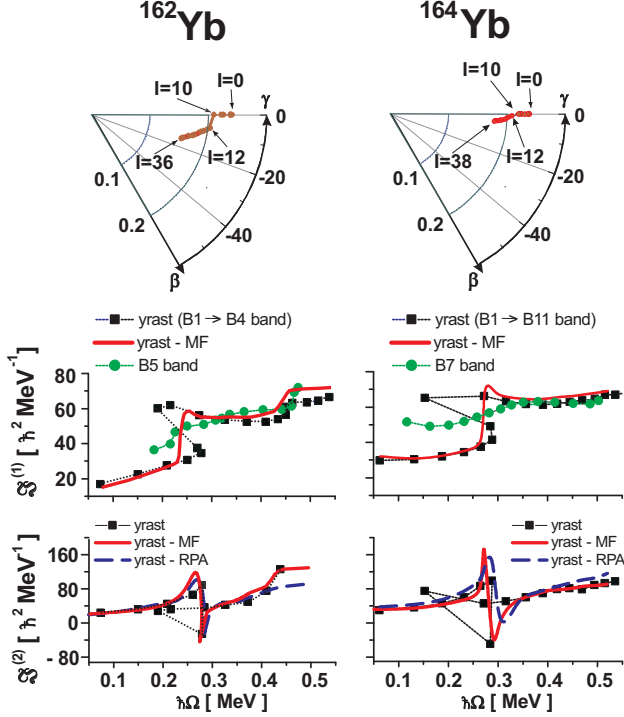


FIG. 3: (Color online) ^{162}Yb (left) and ^{164}Yb (right). Top panels: equilibrium deformations in β - γ plane as a function of the angular momentum $I = \langle \hat{J}_x \rangle - 1/2$ (in units of \hbar). Middle panels: the kinematic $\mathfrak{I}^{(1)}(\Omega) = \langle \hat{J}_x \rangle / \Omega$ momenta of inertia. Filled square (circle) is used for experimental positive (negative) parity lowest states. Different symbols display the experimental data associated with B1, B2...bands (the band labels are taken in accordance with the definitions given in Ref.12). Bottom panels: the dynamic $\mathfrak{I}^{(2)}(\Omega)$ momenta of inertia are compared with the corresponding experimental values (filled squares). Experimental values are connected by thin line to guide eyes. The calculated values of the kinematic (middle) and dynamic (bottom) momenta of inertia for the yrast line are connected by a solid line. The dashed line displays the behavior of the Thouless-Valatin moment of inertia (bottom). All results are obtained within the cranked Nilsson plus RPA (CRPA) approach.

tency between the mean field and the RPA results was achieved by varying the strength constants of the pairing and multipole interactions in the RPA (see Ref.9) to fulfill the conservation laws for both signatures and both parities

$$\begin{aligned} \left[\hat{H}_\Omega(\pi_{r=+}), \hat{N}_\tau \right] &= 0, & \left[\hat{H}_\Omega(\pi_{r=+}), \hat{P}_x \right] &= 0, \\ \left[\hat{H}_\Omega(\pi_{r=+}), \hat{J}_x \right] &= 0, & \left[\hat{H}_\Omega(\pi_{r=+}), \hat{\Gamma}^\dagger \right] &= \hbar\Omega\hat{\Gamma}^\dagger, \end{aligned} \quad (3)$$

where $\hat{\Gamma}^\dagger = (\hat{J}_z + i\hat{J}_y) / \sqrt{2\langle \hat{J}_x \rangle}$. It results in the sep-

aration of physical modes (excitations) from those that are related to the symmetries broken by the mean field. Two Goldstone modes are associated with the violation of the particle number (for protons and for neutrons). The other two Goldstone modes are related to the translational and spherical symmetries of the mean field. The last equation yields a negative signature solution $\hbar\Omega$, a collective rotational mode arising from the symmetries broken by the external rotational field. We recall that the decoupling of \hat{P}_y and \hat{P}_z components of the center of mass operator from physical modes is uniquely defined in the cranking model with a signature and a parity symmetry [14]. The constraint satisfaction of the translational symmetry related to the operator \hat{P}_x determines, therefore, the isoscalar dipole strength solely and also guarantees the decoupling of the spurious center of mass motion from physical modes. This is especially important for the calculations of $B(E1)$ -transitions. For the isovector dipole coupling strength we adopt the standard value $\chi_1 = \pi V_1 / A \langle \hat{r}^2 \rangle$ with $V_1 = 130\text{MeV}$ [1]. The self-consistent octupole strength constants obtained for the anisotropic harmonic oscillator [15] are used in our calculations for octupole excitations, taking into account a rotational dependence of different mean field values in the original expression. By virtue of these constants we nicely reproduce the experimental octupole Routhians (see below).

The different response on the rotation can be understood from the analysis of excited states. To this aim we define the experimental excitation energy in the rotating frame $\hbar\omega_\nu(\Omega)_{exp} = R_\nu(\Omega) - R_{yr}(\Omega)$ as a function of the rotational frequency Ω [16]. Here, the Routhian function $R_\nu(\Omega) = E_\nu(\Omega) - \hbar\Omega I_\nu(\Omega)$. The experimental states are classified by the parity $\pi = \pm$ and a quantum number α which is equivalent to our signature r (see Figs.4,6). The positive signature states ($r = +1$) correspond to $\alpha = 0$ which characterizes rotational bands with even spin in even-even nuclei. The negative signature states ($r = -1$) correspond to $\alpha = 1$ and are associated with odd spin states in even-even nuclei. The energy $\hbar\omega_\nu(\Omega)_{exp}$ can be compared with the RPA results, $\hbar\omega_\nu(\Omega)$, calculated at a given rotational frequency. The agreement between our results and experimental data indicates that quadrupole deformation (axial and nonaxial) is a major factor that determines the evolution of the mean field till $\hbar\Omega \approx 0.6(0.45)\text{MeV}$ in ^{164}Yb (^{162}Yb).

In ^{162}Yb the band B4 crosses the band B1 at the rotational frequency $\hbar\Omega = 0.265\text{MeV}$ (a transition point) and becomes the yrast one for $\hbar\Omega > 0.265\text{MeV}$. The change of the yrast line structure produces the backbending (see Fig.3). It should be emphasized that the potential-energy surfaces are very shallow. The deformations shown in Fig.3 should be not taken as precise predictions, since even before the transition point the yrast states may possess small ($\sim 1^0 - 3^0$) γ -deformation (see also Refs.17, 18). To elucidate the structure near the transition point we trace the rotational evolution of the CRPA solutions and the lowest two-quasiparticle

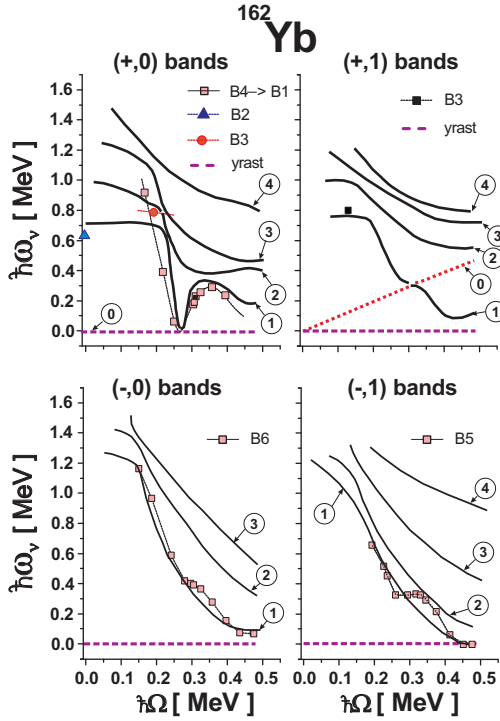


FIG. 4: (Color online) ^{162}Yb . The rotational evolution of CRPA solutions: the positive (negative) signature ones with even (odd) spins are displayed on left (right) panels. Number in a circle denotes the RPA solution number : 1 is the first $\nu = 1$ RPA solution *etc.* Different symbols display the experimental data associated with B1,B2...bands. The yrast line position denoted as "0" (top, left) is displayed by dashed line on all panels. Top panels: positive parity $\pi = +$ solutions. The redundant mode (right) $\omega_\nu = \Omega$ is denoted as "0" and is displayed by dotted line. Bottom panels: negative parity $\pi = -$ solutions.

poles. At $\Omega = 0$ each quasiparticle orbital (routhian) is characterized by asymptotic Nilsson quantum numbers. These numbers are irrelevant, however, in the rotating case and are used only for convenience. The first positive parity and signature RPA solution (see Fig.4, top left panel) may be identified with β -excitations at $\hbar\Omega \leq 0.2\text{MeV}$. The increase of the rotational frequency leads to a strong mixing between γ - (the second RPA solution at low spins) and β -excitations. At the transition point from an axial to nonaxial rotations, $\hbar\Omega \approx 0.26\text{MeV}$, a two-quasiparticle neutron component $3/2[651]3/2[651]$ dominates in the quadrupole phonon structure ($\sim 92\%$). This fact suggests that the alignment of a pair $i_{13/2}$ is the main mechanism that drives the nucleus to triaxial shapes. The first negative signature RPA solution (Fig.4, top right panel) carries the properties of a gamma-vibrational mode (with odd spins) till $\hbar\Omega \approx 0.28\text{MeV}$ and does not lead to any instability.

From Fig.4 (bottom panel, right) one observes that the first negative signature and parity RPA (octupole) solution tends to zero. Almost a zero energy gap between the negative parity band (B5) and the yrast line

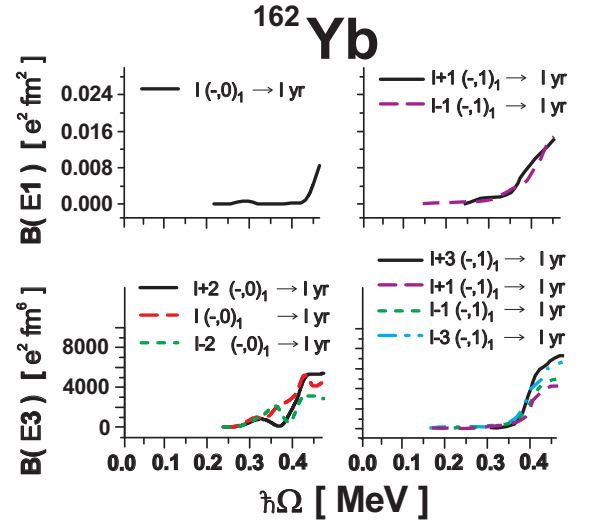


FIG. 5: (Color online) ^{162}Yb . Reduced $B(E1)$ - and $B(E3)$ -transition probabilities from the lowest negative parity one-phonon states to the yrast states. We used the effective proton (neutron) charge $e = N/A(-Z/A)$ for the calculation of $B(E1)$ -transitions, while only the proton contribution is taken into account for the $B(E3)$ -transitions. Left(right) panels correspond to the transition with ΔI even (ΔI odd). All results are obtained within the CRPA approach.

is also observed at $\hbar\Omega \geq 0.45\text{MeV}$. The collectivity of the lowest negative parity RPA solutions of both signatures increases noticeably with the increase of the rotational frequency. Results for reduced $B(E1)$ - and $B(E3)$ -transition probabilities evidently demonstrate the onset of octupole correlations at $\hbar\Omega > 0.3\text{MeV}$ (see Fig.5). For example, $B(E3, \Delta I = 3)$ -transition probability increases from ~ 0.7 W.u. at $\hbar\Omega \approx 0.3\text{MeV}$ to ~ 4.5 W.u. at $\hbar\Omega \approx 0.45\text{MeV}$ (here W.u. is the Weisskopf unit). Several two-quasiparticle components originated from $h_{11/2}$ and $g_{7/2}$ subshells for protons and $i_{13/2}$ and $h_{9/2}$ subshells for neutrons contribute to the collectivity of the lowest negative parity one-phonon states. The maximal weight of two-quasiparticle components is $\sim 65\%$. All these features reveal the nature of a shape transition at $\hbar\Omega \sim 0.45\text{MeV}$. The onset of the static octupole deformations becomes feasible, since the instability point found in the CRPA approach coincides with the result of the Skyrme mean field calculations (see Fig.1). These results suggest that the octupole deformations are due to the octupole phonon condensation at fast rotation.

In ^{164}Yb (see Fig.6), there are observed 15 rotational bands so far [12]. The positive signature family (with even spin) is comprised of B1, B2, B8, B9, B10, B11 bands of positive and B3, B4, B5 bands of negative parities. The negative signature family (with odd spins) includes B2, B12, B13, B14, and B6, B7, B15 of positive and negative parity bands, respectively. At $\hbar\Omega \approx 0.27\text{MeV}$ the band B11 crosses the ground band B1. This crossing gives rise to the backbending (see Fig.3). According to our analysis, the first positive parity and signa-

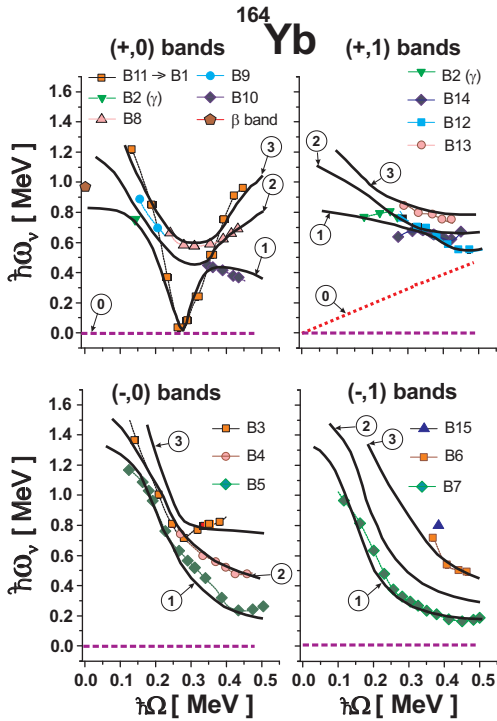


FIG. 6: (Color online) ^{164}Yb . Similar to Fig.4.

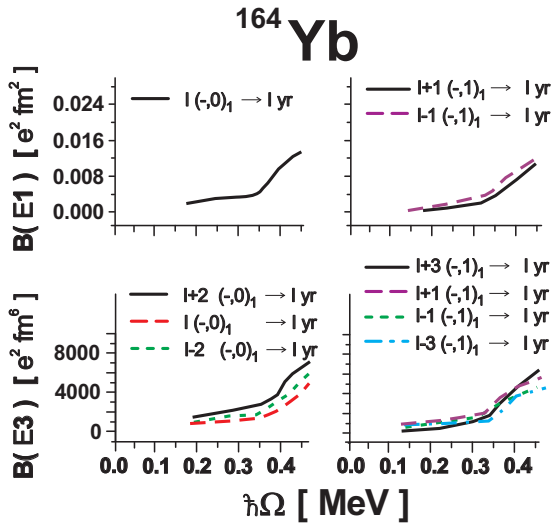


FIG. 7: (Color online) ^{164}Yb . Similar to Fig.5.

ture RPA solution (see Fig.6, top left panel) may be identified with γ -excitations at small rotation $\hbar\Omega \leq 0.2\text{MeV}$. The rotation induces a strong mixing between γ - and β -excitations (the second RPA solution at low spins). Although the pattern is similar to the one of ^{162}Yb , β - and γ - vibrations are interchanged at small rotation. At $\hbar\Omega \approx 0.27\text{MeV}$ the transition from an axial to nonax-

ial rotations is determined by two-quasiparticle neutron component from $i_{13/2}$ subshell. A good agreement between data and our results implies that quadrupole degrees of freedom dominate in this domain of rotational frequency values. The negative parity RPA solutions of both signatures (see Fig.6) decrease with the rotational frequency. The RPA results reproduce with a good accuracy the rotational behaviour of the negative parity states, especially, the lowest one. While the octupole phonons are of collective nature (the maximal component is $\sim 75\%$), the quadrupole deformed field remains stable, even at very high spins. The growing octupole collectivity is exhibited in the increasing dipole and octupole transitions from the negative-parity one phonon states at $\hbar\Omega > 0.3\text{MeV}$ (see Fig.7). In particular, $B(E3, \Delta I = 3)$ -transition probability increases from ~ 1.2 W.u. at $\hbar\Omega \approx 0.3$ MeV to ~ 4.4 W.u. at $\hbar\Omega \approx 0.45$ MeV. In contrast with ^{162}Yb , all negative parity solutions are nonzero at $\hbar\Omega \leq 0.6\text{MeV}$. Octupole correlations are unable to break the reflection symmetry in ^{164}Yb , which elucidates the result of Skyrme calculations (see Fig.1).

Summarizing, we found that the internal structure of the low-lying excited ($\pi = +, r = +1$) band, which crosses the ground band, has almost a pure two-quasiparticle character originating from $i_{13/2}$ neutron subshell, in agreement with the prediction of the phenomenological analysis [17]. In both nuclei the rotation produces a profound affect on shell structure inducing noticeable octupole correlations at high spins. At $\hbar\Omega > 0.3\text{MeV}$ we predict the formation of octupole bands with strong $B(E1)$ - and $B(E3)$ - transitions to the yrast line (see Figs.5,7). We found that at $\hbar\Omega \approx 0.45\text{MeV}$ the octupole phonon solution vanishes in the rotating frame in ^{162}Yb . It results in the onset of the degeneracy between the lowest negative parity and negative signature band and the positive parity and positive signature yrast line. This mechanism explains the spontaneous breaking of reflection symmetry of the rotating mean field with Skyrme interaction (see Fig.1). In contrast, in ^{164}Yb the octupole correlations manifest themselves as a low-lying octupole vibrations of the quadrupole deformed rotating nucleus, in agreement with the Skyrme results.

Acknowledgments

This work is a part of the research plan MSM 0021620859 supported by the Ministry of Education of the Czech Republic and by the project 202/06/0363 of Czech Grant Agency. It is also partly supported by Grant No. FIS2005-02796 (MEC, Spain). R. G. N. gratefully acknowledges support from the Ramón y Cajal programme (Spain).

[1] A. Bohr and B. R. Mottelson, *Nuclear Structure* Vol. II (Benjamin, New York, 1975).

[2] see, for example, S. Zhu *et al.*, Phys. Lett. B 618 (2005)

- 51 ; P. Mason *et al.*, Phys. Rev. C 72 (2005) 064315 ; M. E. Debray *et al.*, Phys. Rev. C 73 (2006) 024314 ; Y. J. Chen *et al.*, Phys. Rev. C 73 (2006) 054316.
- [3] see for a review P. Butler and W. Nazarewicz, Rev. Mod. Phys. 68 (1996) 349.
- [4] F. Garote, J. L. Egido, and L. M. Robledo, Phys. Rev. Lett 80 (1998) 4398.
- [5] M. Yamagami and K. Matsuyanagi, Nucl. Phys. A 672 (2000) 123.
- [6] T. Tanaka, R. G. Nazmitdinov, and K. Iwasawa, Phys. Rev. C 63 (2001) 034309.
- [7] A. Tsvetkov, J. Kvasil, and R. G. Nazmitdinov, J. Phys. G: Nucl. Part. Phys. 28 (2002) 2187.
- [8] J. Dobaczewski and J. Dudek, Comp. Phys. Comm. 131 (2000) 163.
- [9] J. Kvasil and R. G. Nazmitdinov, Phys. Rev. C **69** (2004) 031304(R); Pis'ma v ZhETF 83 (2006) 227 [JETP Lett. 83 (2006) 187]; Phys. Rev. C 73 (2006) 014312.
- [10] J. Kvasil, N. Lo Iudice, V. O. Nesterenko, and M. Kopál, Phys. Rev. C 58 (1998) 209.
- [11] R. G. Nazmitdinov, D. Almeded, and F. Dónau, Phys. Rev. C 65 (2002) 041307(R).
- [12] <http://www.nndc.bnl.gov/nudat2/>
- [13] I. Hamamoto, Nucl. Phys. A 271 (1976) 15.
- [14] S. Cwiok, J. Kvasil, and B. Choriev, J. Phys. G: Nucl. Phys. 10 (1984) 903.
- [15] H. Sakamoto and T. Kishimoto, Nucl. Phys. A 501 (1989) 205.
- [16] R. G. Nazmitdinov, Yad. Fiz. 46 (1987) 732 [Sov. J. Nucl. Phys. 46 (1987) 412].
- [17] S. Frauendorf and F. R. May, Phys. Lett. B 125 (1983) 245.
- [18] J. L. Egido, H. J. Mang, and P. Ring, Nucl. Phys. A 339 (1980) 390; R. Bengtsson, Yong-Shou Chen, Jing-Ye Zhang, and S. Åberg, Nucl. Phys. A 405 (1983) 221; Y. R. Shimizu and K. Matsuyanagi, Prog. Theor. Phys. 71 (1984) 960.